Measuring the top quark Yukawa coupling at a linear e^+e^- collider

Howard Baer
Physics Department, Florida State University, Tallahassee, Florida 32306

Sally Dawson
Physics Department, Brookhaven National Laboratory, Upton, New York 11973

Laura Reina
Physics Department, Florida State University, Tallahassee, Florida 32306

(Received 21 June 1999; published 29 November 1999)

The cross section for the reaction $e^+e^-\to t\bar{t}H$ depends sensitively on the top quark Yukawa coupling λ_t. We calculate the rate for $t\bar{t}H$ production, followed by the decay $H\to b\bar{b}$, for a standard model Higgs boson with 100 GeV$\leqslant m_H \leqslant$130 GeV. We interface with ISAJET to generate QCD radiation, hadronization and particle decays. We also calculate the dominant $t\bar{t}b\bar{b}$ backgrounds from electroweak and QCD processes. We consider both semileptonic and fully hadronic decays of the $t\bar{t}$ system. In our analysis, we attempt a full reconstruction of the top quark and W boson masses in the generated events. The invariant mass of the remaining b jets should show evidence of Higgs boson production. We estimate the accuracy with which λ_t can be measured at a linear e^+e^- collider. Our results, including statistical but not systematic errors, show that the top quark Yukawa coupling can be measured to 6–8 % accuracy with 1000 fb^{-1} at $E_{\rm c.m.}=1$ TeV, assuming 100% efficiency for b-jet tagging. The accuracy of the measurement drops to 17–22 % if only a 60% efficiency for b tagging is achieved.

PACS number(s): 14.80.Bn, 12.38.Bx, 13.85.Lg, 14.65.Ha

I. INTRODUCTION

One of the most important challenges facing the next generation of accelerators is the untangling of the mechanism of electroweak symmetry breaking. In the optimistic scenario where a Higgs boson is discovered at the CERN e^+e^- collider LEP2, the Fermilab Tevatron, or the CERN Large Hadron Collider (LHC), a major goal of a high energy e^+e^- collider becomes the measurement of the Higgs boson couplings to the fermions and gauge bosons. These couplings are uniquely predicted in the standard model (SM), but can be significantly different in extentions such as supersymmetric models. A measurement of the Higgs boson couplings can therefore discriminate between various alternatives to the standard model.

The couplings of the Higgs boson to the gauge bosons can be measured in a straightforward manner through the associated production processes, $e^+e^-\to ZH$, $q\bar{q}'\to W^\pm H$, and $q\bar{q}\to ZH$, and through vector boson fusion, $W^+W^-\to H$ and $ZZ\to H$. The couplings of the Higgs boson to fermions are more difficult to measure, however. In the standard model, the fermion–Higgs-boson couplings are completely determined in terms of the fermion masses. For a generic quark, Q, the $Q\bar{Q}H$ coupling is given by

$$\lambda_Q = -\frac{M_Q}{v}, \tag{1.1}$$

where $v=(\sqrt{2}G_F)^{-1/2}$ and so the top-quark–Higgs-boson Yukawa coupling is much larger than any other Yukawa coupling.

The process $e^+e^-\to t\bar{t}H$ provides a direct mechanism for measuring the top-quark–Higgs-boson Yukawa coupling [1,2]. This process proceeds mainly via γ and Z exchange, with the Higgs boson radiated from the top quark. This contribution is directly proportional to λ_t^2. There is also a contribution from the Higgs boson coupling to the exchanged Z, but this contribution is subdominant and so does not upset the interpretation of the $e^+e^-\to t\bar{t}H$ process as a measurement of the top-quark–Higgs-boson Yukawa coupling.

At a high energy e^+e^- collider with $E_{\rm c.m.}=500$ GeV, the process $e^+e^-\to t\bar{t}H$ is sensitive to Higgs bosons in the mass region 100 GeV$\sim m_H \sim$130 GeV. The current limit on m_H from LEP2 is $m_H>95.2$ GeV [3]. This Higgs boson mass regime is favored by calculations comparing precision electroweak data to standard model predictions [4]. In addition, the lightest Higgs boson of supersymmetric models (which for many models behaves indistinguishably from the SM Higgs boson) ought to have mass less than typically 130 GeV [5]. In the interesting 100–130 GeV mass region, the Higgs boson will decay predominantly to $b\bar{b}$ pairs and so the final state of interest will be $t\bar{t}b\bar{b}$. Since the top quark decays to a W boson and a b quark, the final state will contain at least four b quarks plus two W bosons. Although the rate is small (on the order of a few femtobarns), the signature is quite spectacular.

There are two major sources of background to the $t\bar{t}b\bar{b}$ final state [6]. There is a large QCD background, coming primarily from the process $e^+e^-\to t\bar{t}g^*$, with the gluon decaying to a $b\bar{b}$ pair. The $b\bar{b}$ pairs resulting from the gluon

splitting tend to peak at low values of the $b\bar{b}$ invariant mass. There is also an electroweak (EW) background, of which the dominant contribution is $e^+e^- \to Zt\bar{t}$. Although the EW background is formally smaller than the QCD background, it is more problematic since the $Z \to b\bar{b}$ decay resonates in close proximity to the expected Higgs signal. We compute these backgrounds and estimate the resulting precision which can be obtained on λ_t.

The $O(\alpha_s)$ cross section for $e^+e^- \to t\bar{t}H$ has been calculated in Refs. [7,8]. In this paper, we work entirely with tree level cross sections, for consistency with the background predictions. The dominant effect of QCD corrections will be to increase the precision of signal and background total cross section calculations, so that results from this paper can be appropriately rescaled once the QCD corrected background rates are available.

Recently, Moretti has presented parton-level calculations of both signal and background processes for the semileptonic final state [6]. We have confirmed both his signal and background results at the parton level. In this paper, we extend our programs to include parton showering, hadronization and particle decays. We consider both the semileptonic final state

$$e^+e^- \to (bl\nu) + (bq\bar{q}') + (H \to b\bar{b})$$

and the fully hadronic final state

$$e^+e^- \to (bq_1\bar{q}_1') + (bq_2\bar{q}_2') + (H \to b\bar{b}).$$

In our approach, we rely on a full reconstruction of the various top quark, *W*-boson and Higgs boson invariant masses in the events, which should lend confidence that the appropriate signal and background processes are in fact being seen.

Similar analyses of top quark Yukawa coupling measurements have recently been presented at conferences. A recent analysis of the signal and background for $t\bar{t}H$ production and decay for both semileptonic and hadronic channels has been presented by Juste and Merino using a neural net approach [9]. An independent analysis is also being carried out by the authors of Ref. [10].

The associated $e^+e^- \to Q\bar{Q}H_i$ process (for $Q=t,b$) is also of interest in supersymmetric models [1,11,12]. In such models, there are five Higgs bosons, H_i, which can be produced and the couplings of the Higgs bosons may differ significantly from those of the standard model. In particular, the coupling of at least one of the Higgs bosons to the b quark may be enhanced. In addition, because of the tri-linear coupling of the Higgs bosons to a scalar and a pseudoscalar, in such models the $b\bar{b}H$ production receives large resonance contributions not present in the standard model. These models offer a rich phenomenology, but will not be considered here.

In this paper, Sec. II contains a description of some of our calculational details. Section III presents results for a linear e^+e^- collider operating at $E_{\text{c.m.}}=500$ GeV, while Sec. IV shows corresponding results for $E_{\text{c.m.}}=1$ TeV. In Sec. V, we present a discussion and some conclusions.

II. CALCULATIONAL DETAILS

The starting point for our signal and background calculations is the calculation of the corresponding squared matrix elements for the relevant subprocesses. For these, we use the computer program MADGRAPH [13] and the HELAS subroutines [14]. We compute[1]

$$e^+e^- \to t\bar{t}H \quad (5 \text{ diagrams}),$$

$$e^+e^- \to t\bar{t}b\bar{b} \quad (\text{EW: } 35 \text{ diagrams}),$$

and

$$e^+e^- \to t\bar{t}b\bar{b} \quad (\text{QCD: } 8 \text{ diagrams}).$$

In the QCD contribution, we have taken $\alpha_s(M_Z)=.118$. We notice that, with respect to Ref. [9], our background calculation includes the *Z*-boson spin correlation effects for the electroweak background. Moreover the dominant QCD background is fully simulated.[2]

The squared matrix elements are integrated via Monte Carlo simulations over phase space, and the total cross sections and distributions agree with the results of Moretti [6]. Next, we interface our parton-level programs with the event generator ISAJET [15] to allow for parton showers, hadronization and particle decays. We neglect initial state bremsstrahlung and beamstrahlung effects. For our analysis, these effects should mainly lead to a small rescaling of both the signal and background production cross sections. We also neglect the spin correlation of the top quark between production and decay, but expect this to be a small effect as well.

In our analysis, we use the ISAJET toy detector simulation program ISAPLT. We assume calorimetry in the range $-4 < \eta < 4$, with cell size $\Delta\eta \times \Delta\phi = 0.1 \times 0.262$. We take the electromagnetic energy resolution to be $0.15/\sqrt{E} \oplus 0.01$ and the hadronic calorimeter resolution to be $0.5/\sqrt{E} \oplus 0.02$ (E in GeV). Calorimeter cells are coalesced in towers of $\Delta R = \sqrt{(\Delta\eta)^2 + (\Delta\phi)^2} = 0.5$ using the jet finding algorithm GETJET. Hadronic clusters with $E_T(j) > 15$ GeV are called jets. Leptons (e's or μ's) with p_T of 5 GeV or more are

[1]Graphs involving the Higgs boson have been removed from the EW background to avoid double counting.

[2]Additional backgrounds can occur, for instance, from direct $t\bar{t}$ production where two or more light quark or gluon jets are radiated. The tree level cross section for $t\bar{t}$ production is 561 fb (173 fb) at $E_{\text{c.m.}}=500(1000)$ GeV. A rough estimate including a factor of 0.1 for each extra QCD jet plus a probability of 0.01–0.001 for a light quark or gluon jet to fake a tagged b jet shows that this rate is well below the backgrounds we have calculated. In addition, the background from $t\bar{t}c\bar{c}$ production should be well below the background from $t\bar{t}b\bar{b}$ production since the charm jets will have a much lower probability to be tagged as a b jet.

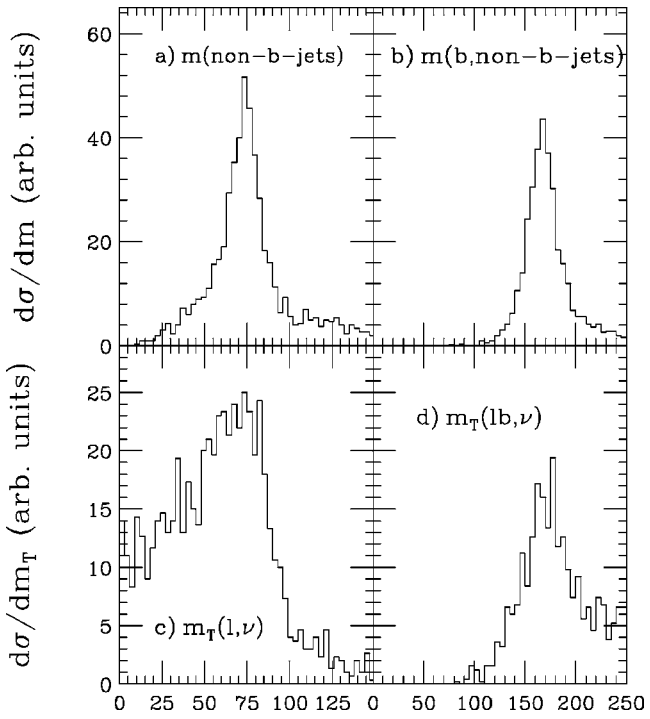

FIG. 1. For $t\bar{t}H \to l+4b+\text{jets}+\not{E}_T$ events, with $m_H = 120$ GeV and $E_{\text{c.m.}} = 1$ TeV, we plot distributions in (a) invariant mass of non-b jets, (b) invariant mass of non-b jets plus the b jet which gives a mass closest to m_t, (c) isolated lepton plus missing energy transverse mass, and (d) isolated lepton plus b jet plus missing energy cluster transverse mass for the b jet which most closely reconstructs m_t.

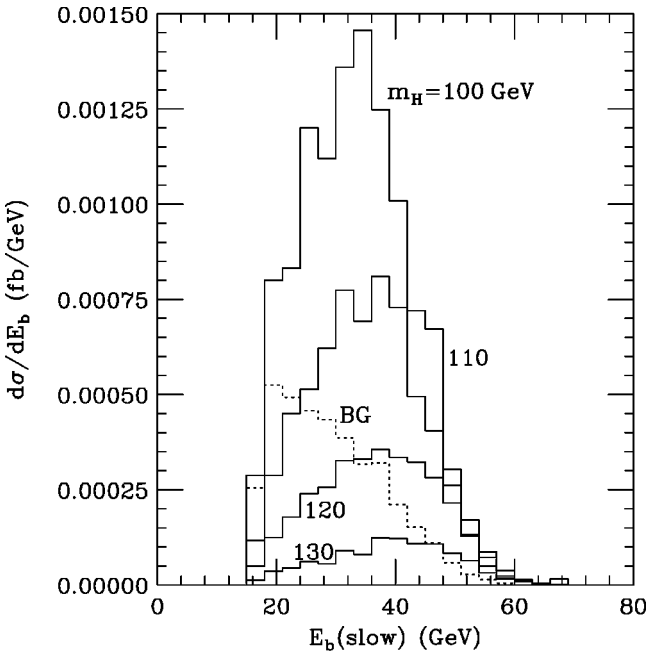

FIG. 2. Energy distribution for the slowest of four b jets in $l+4b+\text{jets}+\not{E}_T$ events at the NLC, at $E_{\text{c.m.}} = 500$ GeV.

considered to be isolated if the hadronic E_T in a cone about the lepton of $\Delta R = 0.4$ is less than 2 GeV. Jets are classified as b jets with a tag efficiency of ϵ_b if they coincide with an original b parton within an angle $\Delta R = 0.4$.

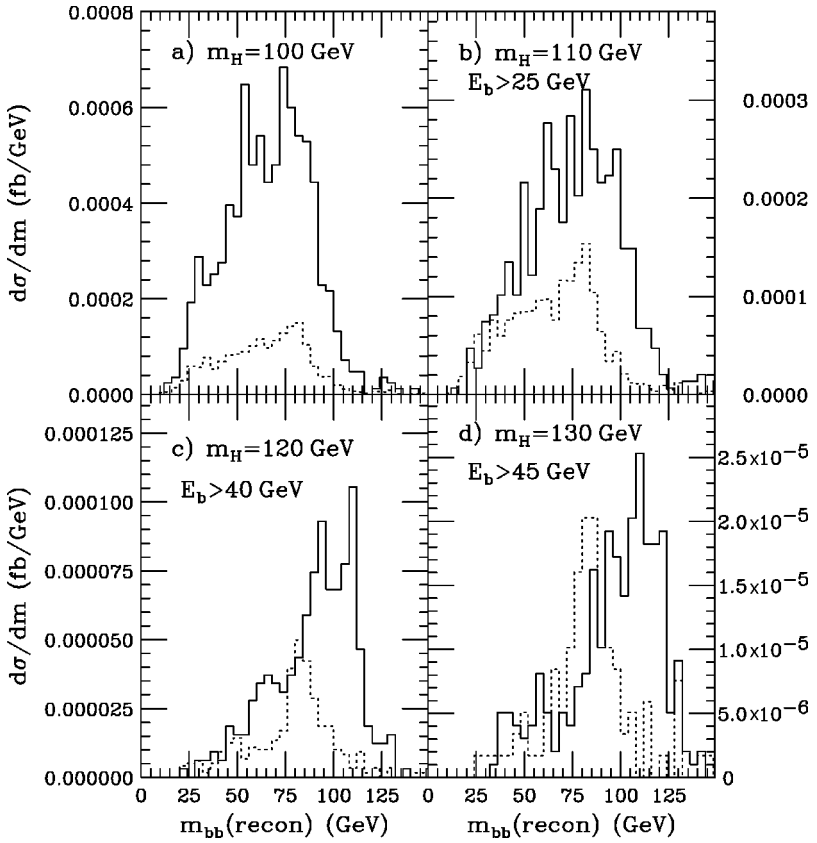

FIG. 3. Distribution in $b\bar{b}$ invariant mass for the two remaining b jets after top quark mass reconstruction, for the semileptonic events at $E_{\text{c.m.}} = 500$ GeV. The signal is solid, while the sum of EW and QCD backgrounds is dashed.

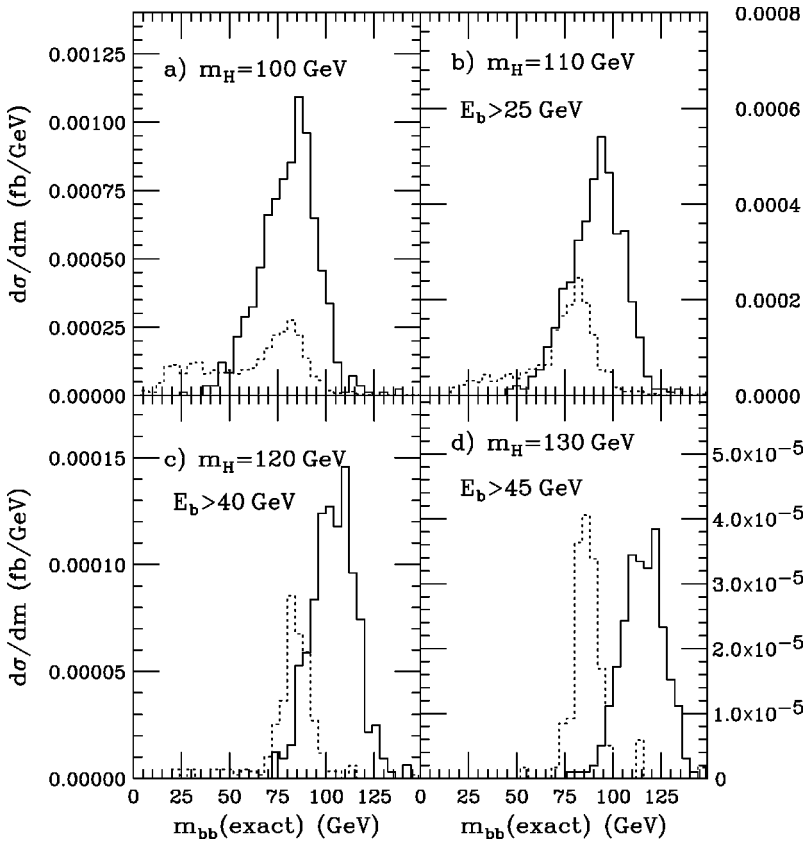

FIG. 4. Distribution in $b\bar{b}$ invariant mass for the two correctly identified non-top-quark b jets, using generator information for semileptonic events, at $E_{\text{c.m.}}=500$ GeV. The signal is solid, while the sum of EW and QCD backgrounds is dashed.

III. OBSERVABILITY AT $E_{\text{c.m.}}=500$ GeV

A. Semileptonic channel

To examine events in the semileptonic channel, we require

one and only one isolated e or μ with $E>15$ GeV,

$\not{E}_T>15$ GeV,

exactly four tagged b jets,

$\geqslant 2$ non-b jets,

$60<m(\text{non-}b \text{ jets})<90$ GeV (consistent with M_W).

The number of events expected for 1000 fb^{-1} of integrated luminosity at $E_{\text{c.m.}}=500$ GeV is shown before and after these cuts in the first two rows of Table I. For the time being, we take $\epsilon_b=1$. Already at this stage we see a huge reduction in the QCD background. The major QCD background reduction comes from the requirement of exactly 4 b jets in the final state: for this background, the b's from $g^* \to b\bar{b}$ are usually relatively soft and not well separated in angle, so only rarely do we get four distinct b jets from this process. The signal is already well in excess of background for $m_H=100$ and 110 GeV, and ranges from 3 to 33 events for the m_H values we have chosen. An integrated luminosity of order 1000 fb^{-1} will be essential for this measurement at $E_{\text{c.m.}}=500$ GeV.

TABLE I. The $l+4b+\text{jets}+\not{E}_T$ final state at $E_{\text{c.m.}}=500$ GeV: number of events for different selection cuts, assuming 10^3 fb^{-1} of integrated luminosity and $\epsilon_b=1$. All energies and masses are in GeV. $m(\text{rec})$ is the invariant mass of the $b\bar{b}$ system remaining after reconstructing the top quark masses. $m(\text{ex})$ is the invariant mass of the $b\bar{b}$ system coming from the Higgs boson decay artificially selected using Monte Carlo information. E_b is the energy of the slowest b jet.

Channel	$H(100)$	$H(110)$	$H(120)$	$H(130)$	$t\bar{t}b\bar{b}$(EW)	$t\bar{t}b\bar{b}$(QCD)
Total	960	540	250	80	170	840
$l+4b+\text{jets}+\not{E}_T$	33.6	19.3	9.8	3.2	6.7	4.6
$E_b>25$, $m(\text{rec})>50$	—	13.7	—	—	4.2	0.9
$E_b>40$, $m(\text{rec})>90$	—	—	2.2	—	0.35	0.05
$E_b>45$, $m(\text{rec})>90$	—	—	—	0.7	0.15	0.034
$E_b>25$, $m(\text{ex})>85$	—	11.2	—	—	1.6	0.13
$E_b>40$, $m(\text{ex})>90$	—	—	3.5	—	0.3	0.017
$E_b>45$, $m(\text{ex})>95$	—	—	—	1.0	0.034	0.017

TABLE II. The $l+4b+\text{jets}+\not{E}_T$ channel at $E_{\text{c.m.}}=500$ GeV: estimated error in the top quark Yukawa coupling ($\delta\lambda_t/\lambda_t$), assuming 10^3 fb^{-1} of integrated luminosity and $\epsilon_b=1$ ($\epsilon_b=0.6$).

Channel	$H(100)$	$H(110)$	$H(120)$	$H(130)$
$l+4b+\text{jets}+\not{E}_T$	0.11 (0.31)	0.17 (0.46)	0.29 (0.80)	0.79 (2.2)
$E_b>25$, $m(\text{rec})>50$	—	0.18 (0.49)	—	—
$E_b>40$, $m(\text{rec})>90$	—	—	0.39 (1.09)	—
$E_b>45$, $m(\text{rec})>90$	—	—	—	0.74 (2.05)
$E_b>25$, $m(\text{ex})>85$	—	0.17 (0.47)	—	—
$E_b>40$, $m(\text{ex})>90$	—	—	0.29 (0.80)	—
$E_b>45$, $m(\text{ex})>95$	—	—	—	0.52 (1.46)

At this stage, we can attempt to reconstruct some of the invariant masses that occur in these events. As an example, we show various mass distributions in Fig. 1. These distributions were generated for $m_H=120$ GeV and $E_{\text{c.m.}}=1$ TeV; the results for $E_{\text{c.m.}}=500$ GeV are qualitatively similar. First, in Fig. 1(a), the invariant mass of *all* non-b jets in the events (before imposing the 60–90 GeV cut listed above) is shown. The invariant mass rises to a peak near to, but slightly below, $m(\text{non-}b\ \text{jets})=M_W$. The peak occurs below M_W mainly due to jet activity leaking out of our fixed cone algorithm, so better jet reconstruction algorithms may improve upon this. Some energy loss also occurs due to a restricted detector acceptance. We impose the $60<m(\text{non-}b\ \text{jets})<90$ GeV cut to ensure events consistent with a hadronic W-boson decay.

In Fig. 1(b), we combine the non-b jets with the b jet which most nearly reconstructs the top quark mass. The distribution peaks sharply just below m_t, due in part to missing neutrinos from B-meson cascade decays, along with leakage from the jet cones. In Fig. 1(c), we attempt to reconstruct the other $W\to l\nu$ decay. Beam and bremsstrahlung effects do not allow us to use the beam-beam center-of-mass energy to constrain the z component of missing energy, so we work instead with transverse mass. The transverse mass distribution is shown, and peaks as expected just below $m_T(l,\not{E}_T)=M_W$, with considerable smearing due in part to B and D meson semileptonic decay contamination. Finally, in Fig. 1(d), we reconstruct the $bl+\not{E}_T$ cluster transverse mass. We pick one of the remaining b jets which most nearly reconstructs to $\leqslant m_t$. The peak from the top quark decay is again visible. If our mass reconstruction algorithm has been successful, then the remaining two b jets should reconstruct to m_H for our signal events, but to other values for background events.

At this point, we note that the energy distribution of b jets should vary considerably between signal and background. This should especially hold true for the slowest (least energetic) of the b jets. We plot in Fig. 2 the energy distribution of the slowest of b jets, $E_b(\text{slow})$, at $E_{\text{c.m.}}=500$ GeV, after the above cuts. The dashed histogram for the sum of all background processes peaks at low $E_b(\text{slow})$, while the $E_b(\text{slow})$ distribution for the signal becomes increasingly harder for heavier Higgs boson masses. To gain some improvement in signal-to-background ratio (S/B), we will impose

$E_b(\text{slow})>25$, 40 and 45 GeV

for $m_H=110$, 120 and 130 GeV.

After the above cuts and mass reconstructions, we plot in Fig. 3 the invariant mass of the remaining two b jets. The signal histograms are solid, while the background is dashed. For the $m_H=100$ GeV case, the mass distribution peaks somewhat below 100 GeV with a rather broad smear. In this case, the distribution in energy for b jets from Higgs boson decay is similar to the energy distribution of b jets from top quark decay, so our reconstruction algorithm often fails to select the correct b jets from Higgs boson decay. In addition, neutrinos from B and D meson decay serve to further soften the distribution. As we increase the Higgs boson mass in frames (b)–(d), the signal distribution becomes harder and sharper.

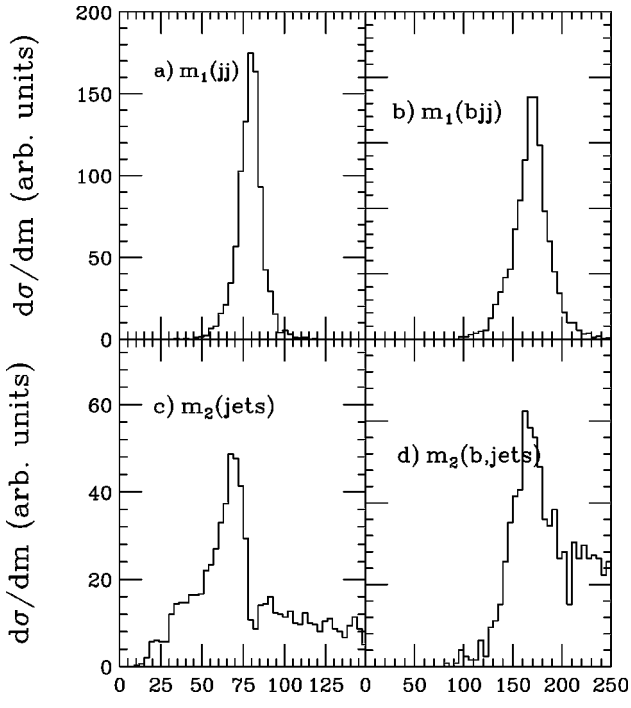

FIG. 5. For $t\bar{t}H\to 4b+\geqslant 4$ jets$+\not{E}_T$ events, with $m_H=120$ GeV and $E_{\text{c.m.}}=1$ TeV, we plot distributions in (a) dijet invariant mass closest to M_W, (b) invariant mass of dijet plus b-jet combination closest to m_t, (c) invariant mass of remaining non-b jets, and (d) invariant mass of remaining non-b jets plus remaining b jet which gives a mass closest to m_t.

TABLE III. The $4b+\geqslant 4$ jets final state at $E_{\text{c.m.}}=500$ GeV: number of events for different selection cuts, assuming 10^3 fb^{-1} of integrated luminosity and $\epsilon_b=1$.

Channel	$H(100)$	$H(110)$	$H(120)$	$H(130)$	$t\bar{t}b\bar{b}$(EW)	$t\bar{t}b\bar{b}$(QCD)
Total	960	540	250	80	170	840
$4b+\geqslant 4$ jets	32.8	19.7	8.8	3.2	5.8	4.7
$E_b>25$, m(rec)>0	—	15.9	—	—	4.4	2.3
$E_b>40$, m(rec)>80	—	—	2.0	—	0.89	0.12
$E_b>45$, m(rec)>90	—	—	—	0.62	0.3	0.017
$E_b>25$, m(ex)>75	—	13.2	—	—	3.3	0.29
$E_b>40$, m(ex)>90	—	—	2.6	—	0.42	0.017
$E_b>45$, m(ex)>90	—	—	—	0.86	0.31	<0.017

For comparison, we show in Fig. 4 the $m(bb)$ distribution using generator information to select the correct b-quark jets. These distributions may be approached, for instance, by using additional information such as the previously measured Higgs boson mass in the reconstruction algorithm. For these cases, the Higgs boson mass peak is more clearly defined, as is the peak in the background from the Z resonance.

Our results for this channel at $E_{\text{c.m.}}=500$ GeV are collected in Tables I and II. The columns labeled with the Higgs boson mass [$H(100)$, etc.] are the signal for $e^+e^-\to t\bar{t}H$, $H\to b\bar{b}$ followed by decays yielding four b-quark jets plus a lepton plus missing energy. The columns labeled $t\bar{t}b\bar{b}$(EW) and $t\bar{t}b\bar{b}$(QCD) give the electroweak and QCD backgrounds respectively.

The first row of Table I gives the total number of $t\bar{t}b\bar{b}$ events before the top quark decays. In the second row we report the number of events reconstructed for the specific channel. By placing cuts on the $m(bb)$ mass distribution, some further improvement in S/B can be gained. We list in the following rows of Table I the events expected after selected cuts on E_b(slow) and $m(bb)$. After cuts, the remaining number of events is between 1 and 34 for 1000 fb^{-1}. Even with this optimistically high luminosity, there is less than one remaining signal event for $m_H=130$ GeV.

In Table II, we show the resulting statistical precision for the measurement of $\delta\lambda_t/\lambda_t$, for $\epsilon_b=1$ and 0.6. The error is calculated assuming a Poisson distribution for both signal and background, and is given by

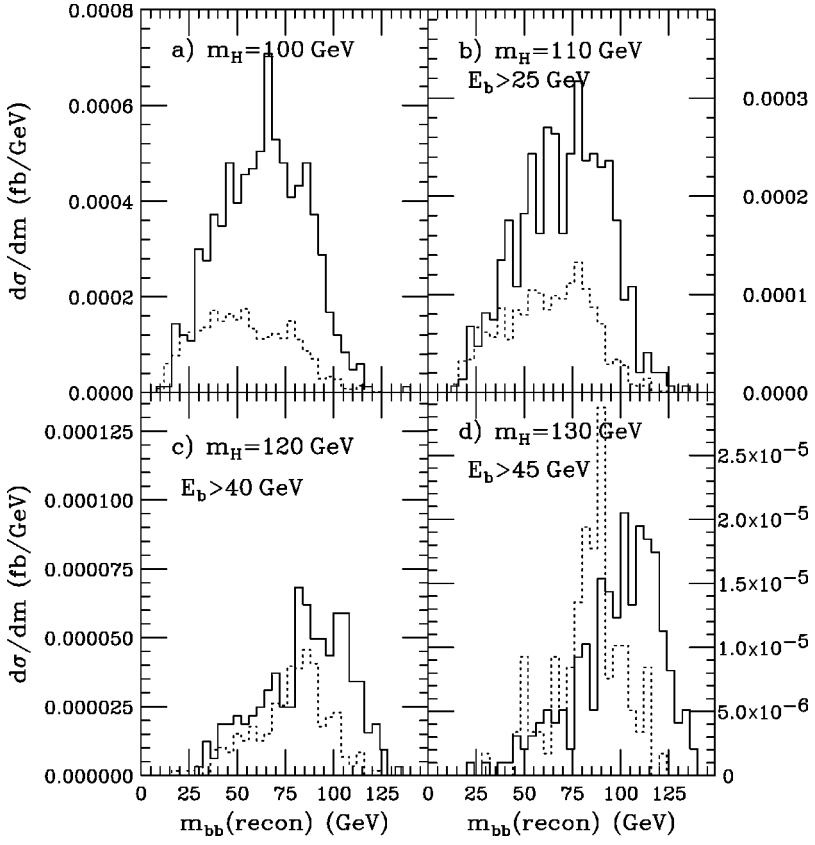

FIG. 6. Distribution in $b\bar{b}$ invariant mass for the two remaining b jets after top quark mass reconstruction at $E_{\text{c.m.}}=500$ GeV, for the hadronic final state. The signal is solid, while the sum of EW and QCD backgrounds is dashed.

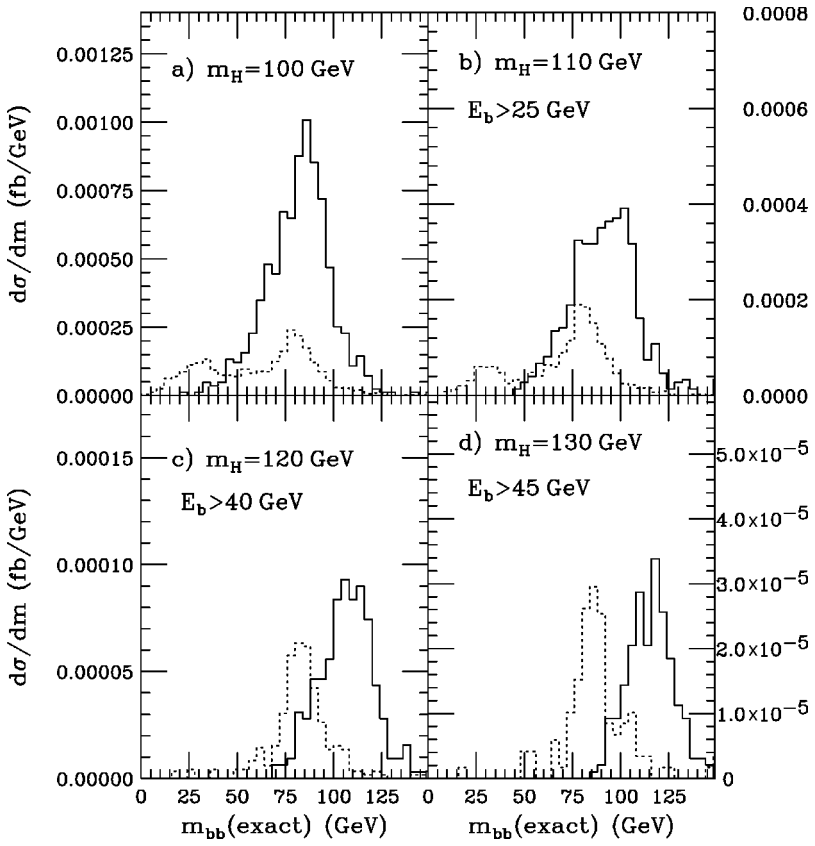

FIG. 7. Distribution in $b\bar{b}$ invariant mass for the two correctly identified non-top-quark b jets, using generator information for hadronic events, at $E_{\text{c.m.}}=500$ GeV. The signal is solid, while the sum of EW and QCD backgrounds is dashed.

$$\frac{\delta\lambda_t}{\lambda_t}=\frac{1}{\sqrt{S}}\sqrt{1+\frac{2B}{S}}, \tag{3.1}$$

where S and B are respectively the number of signal and background events. We have assumed that $\Gamma(H\to b\bar{b})$ will be known precisely from previous measurements at the LHC and Next Linear Collider (NLC), and so the signal rate for $e^+e^-\to t\bar{t}H$, $H\to b\bar{b}$ depends only on λ_t. If high efficiency can be achieved on b-jet tagging, then already at $E_{\text{c.m.}}=500$ GeV the top quark Yukawa coupling can be measured to 11% for $m_H=100$ GeV. This decreases to 31% if only $\epsilon_b=0.6$ is achieved. The precision $\delta\lambda_t/\lambda_t$ becomes rapidly worse as m_H increases beyond 100 GeV. For $m_H=120$ GeV and an integrated luminosity L, we find

$$\frac{\delta\lambda_t}{\lambda_t}\sim 39\%\sqrt{\frac{1000\ \text{fb}^{-1}}{L\epsilon_b^4}},\quad m_H=120\ \text{GeV}. \tag{3.2}$$

It appears that $E_{\text{c.m.}}=500$ GeV is a poor energy for the measurement of the $t\bar{t}H$ Yukawa coupling unless the Higgs boson is ~ 100 GeV. At this energy, the $t\bar{t}H$ system is close to the phase space limit and the parent particles have little kinetic energy, making the kinematic cuts and event reconstruction less effective than at higher energies. In addition, the number of events is too small to obtain a statistically precise measurement for the heavier Higgs boson masses.

B. Hadronic channel

The totally hadronic channel for $e^+e^-\to t\bar{t}H$ has the advantage of initially higher rates than the semileptonic chan-

TABLE IV. The $4b+\geq 4$ jets channel at $E_{\text{c.m.}}=500$ GeV: estimated error in the top quark Yukawa coupling ($\delta\lambda_t/\lambda_t$), assuming 10^3 fb^{-1} of integrated luminosity and $\epsilon_b=1$ ($\epsilon_b=0.6$).

Channel	$H(100)$	$H(110)$	$H(120)$	$H(130)$
$4b+\geq 4$ jets	0.11 (0.31)	0.16 (0.45)	0.31 (0.86)	0.77 (2.13)
$E_b>25$, $m(\text{rec})>50$	—	0.17 (0.47)	—	—
$E_b>40$, $m(\text{rec})>90$	—	—	0.50 (1.39)	—
$E_b>45$, $m(\text{rec})>90$	—	—	—	0.90 (2.50)
$E_b>25$, $m(\text{ex})>85$	—	0.17 (0.47)	—	—
$E_b>40$, $m(\text{ex})>90$	—	—	0.36 (0.99)	—
$E_b>45$, $m(\text{ex})>95$	—	—	—	0.71 (1.96)

TABLE V. The $l+4b+\text{jets}+\not{E}_T$ final state at $E_{\text{c.m.}}=1$ TeV: number of events for different selection cuts, assuming 10^3 fb^{-1} of integrated luminosity and $\epsilon_b=1$.

Channel	$H(100)$	$H(110)$	$H(120)$	$H(130)$	$t\bar{t}b\bar{b}(\text{EW})$	$t\bar{t}b\bar{b}(\text{QCD})$
Total	2420	2080	1690	1210	510	1900
$l+4b+\text{jets}+\not{E}_T$	111	97	81	60	29	32
$m(\text{rec})>60$	104	—	—	—	28	24
$m(\text{rec})>90$	—	77	68	—	17	19
$m(\text{rec})>100$	—	—	—	47	15	18
$m(\text{ex})>70$	97	—	—	—	25	14
$m(\text{ex})>90$	—	68	67	—	7	10
$m(\text{ex})>95$	—	—	—	49	4	9

nel due to the large W boson hadronic branching fraction. However, in attempting mass reconstructions, a greater combinatoric problem is presented since there will now be typically four or more non-b jets in each event, in addition to the four b jets.

For the hadronic channel, we make the following cuts:
exactly zero isolated leptons with $p_T>5$ GeV,
exactly four identified b jets,
$\geqslant 4$ non-b jets .

We then attempt mass reconstruction. In Fig. 5(a), we show the invariant mass of the two non-b jets $m_1(jj)$ that most nearly reconstructs M_W. Again, for illustration, we show these results for $m_H=120$ GeV and $E_{\text{c.m.}}=1$ TeV; results for $E_{\text{c.m.}}=500$ GeV are qualitatively similar. The resonance from the W boson is evident. In Fig. 5(b), we cluster the two jets from Fig. 5(a) with the b jet which most nearly reconstructs m_t; the distribution has the expected peak just below $m_1(bjj)=m_t$. In Fig. 5(c), we plot the invariant mass of *all* the remaining non-b jets. In this case, we again have a peak near $m_2(\text{jets})=M_W$, but with significant smearing below and above the peak. Likewise, in Fig. 5(d) we show the invariant mass of the jets from Fig. 5(c) with the remaining b jet which most nearly reconstructs m_t. The distribution peaks at m_t, but again with significant smearing, especially above $m_2(b,\text{jets})=m_t$. To be consistent with reconstructing a second hadronic W and a second hadronic top quark, we require only events with

$$60<m_2(\text{jets})<90 \text{ GeV}$$

and $125<m_2(b,\text{jets})<200$ GeV.

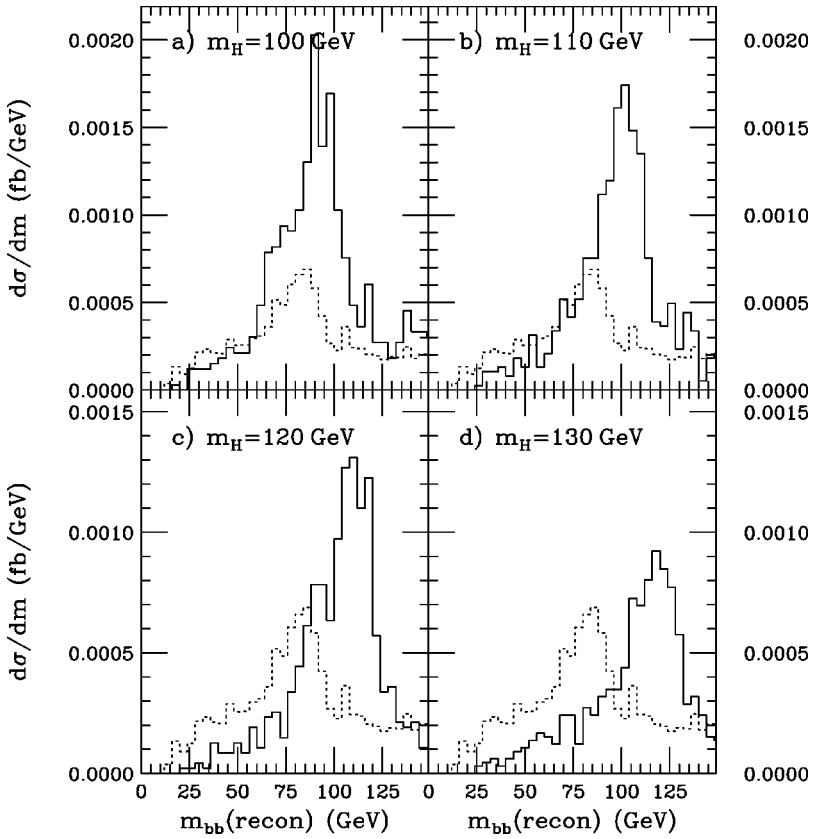

FIG. 8. Distribution in $b\bar{b}$ invariant mass for the two remaining b jets after top quark mass reconstruction, for semileptonic events at $E_{\text{c.m.}}=1$ TeV. The signal is solid, while the sum of EW and QCD backgrounds is dashed.

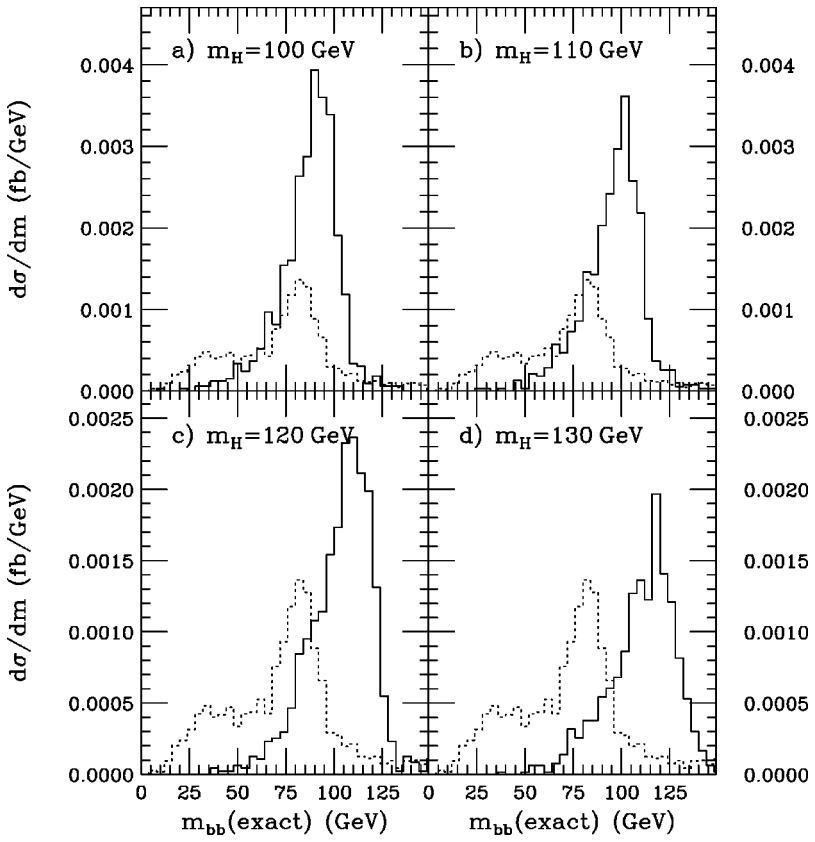

FIG. 9. Distribution in $b\bar{b}$ invariant mass for the two correctly identified non-top-quark b jets, using generator information for semileptonic events, at $E_{\text{c.m.}}=1$ TeV. The signal is solid, while the sum of EW and QCD backgrounds is dashed.

The resulting event rates are listed in Table III, following the same pattern explained in Sec. III A. After these additional cuts, the surviving number of events in 1000 fb^{-1} is surprisingly close to the number of events expected in the semileptonic channel.

At this point, we may apply the same b-jet energy cuts as in the semileptonic case, and plot the mass of the remaining b jets in the events. These results are shown in Figs. 6 and 7 for the remaining b jets and the exact reconstruction, respectively. As before, some improvement in S/B can be made by adopting a $m(bb)$ mass cut. These are listed in Table III, along with the surviving number of events. In a similar fashion to the semileptonic case, we can then extract the error measurements on the top quark Yukawa coupling, and these are listed in Table IV for $\epsilon_b=1$ and 0.6. In the hadronic channel, the results are very similar to the leptonic case, and so will offer an independent confirmation of any sort of top quark Yukawa measurement. Of course, the semileptonic and hadronic channel measurements can be combined to improve the overall precision of the measurement.

IV. OBSERVABILITY AT $E_{\text{c.m.}}=1$ TeV

A. Semileptonic channel

At $E_{\text{c.m.}}=1$ TeV, the total event rates are significantly larger than at $E_{\text{c.m.}}=500$ GeV. Since this energy scale is far above the kinematic limit, there is only a modest sensitivity of the total signal rate to the Higgs boson mass. At $E_{\text{c.m.}}=1$ TeV, the energy distribution of the slowest b jet is not as distinctive as it was in the $E_{\text{c.m.}}=500$ GeV, due mainly to the high momentum of the parent particles that are produced. Hence, we drop the E_b(slow) cut for this energy regime. We

TABLE VI. The $l+4b+\text{jets}+\not{E}_T$ channel at $E_{\text{c.m.}}=1$ TeV: estimated error in the top quark Yukawa coupling ($\delta\lambda_t/\lambda_t$), assuming 10^3 fb^{-1} of integrated luminosity and $\epsilon_b=1$ ($\epsilon_b=0.6$).

Channel	$H(100)$	$H(110)$	$H(120)$	$H(130)$
$l+4b+\text{jets}+\not{E}_T$	0.07 (0.19)	0.08 (0.21)	0.09 (0.24)	0.11 (0.31)
$m(\text{rec})>60$	0.07 (0.19)	—	—	—
$m(\text{rec})>90$	—	0.08 (0.22)	0.09 (0.24)	—
$m(\text{rec})>100$	—	—	—	0.11 (0.31)
$m(\text{ex})>70$	0.07 (0.19)	—	—	—
$m(\text{ex})>90$	—	0.07 (0.21)	0.07 (0.21)	—
$m(\text{ex})>95$	—	—	—	0.09 (0.24)

TABLE VII. The $4b+\geqslant 4$ jets final state at $E_{\text{c.m.}}=1$ TeV: number of events for different selection cuts, assuming 10^3 fb^{-1} of integrated luminosity and $\epsilon_b=1$.

Channel	$H(100)$	$H(110)$	$H(120)$	$H(130)$	$t\bar{t}b\bar{b}$(EW)	$t\bar{t}b\bar{b}$(QCD)
Total	2420	2080	1690	1210	510	1900
$4b+\geqslant 4$ jets	51	48	38	27	12	19
m(rec)>65	43	—	—	—	11	12
m(rec)>75	—	39	—	—	9	11
m(rec)>90	—	—	27	—	6	9
m(rec)>95	—	—	—	19	5	9
m(ex)>65	46	—	—	—	11	8
m(ex)>75	—	41	—	—	9	6
m(ex)>90	—	—	28	—	2	5
m(ex)>95	—	—	—	21	2	4

do adopt the remaining semileptonic cuts from Sec. III and show the resulting signal and background rates in Table V. After selection cuts, about 60 background events should remain while 60–110 signal events would be present, depending on the value of m_H. We apply the same mass reconstruction algorithm as in Sec. III, and plot the invariant mass of the remaining bb pair in Fig. 8 and the mass of the correctly identified bb pair in Fig. 9. The mass reconstruction in Fig. 8 is far sharper than the corresponding plot at 500 GeV. In this case, the large kinetic energy of the parents is transferred to the daughter particles, and wrong mass reconstructions become much more difficult. We may again apply a $m(bb)$ mass cut, as listed in Table V, to improve the S/B ratio. The corresponding precision on the top quark Yukawa coupling measurement is listed in Table VI. Although the contribution of the ZZH-vertex diagram increases at $E_{\text{c.m.}}=1$ TeV with respect to $E_{\text{c.m.}}=500$ GeV, it is still of the order of a few percent and completely negligible in the determination of the error on λ_t.

From Table VI, we see that there will be roughly a 7–9 % measurement of $\delta\lambda_t/\lambda_t$ in the leptonic channels with 1000 fb^{-1} for $\epsilon_b=1$. These results are degraded to 19–24 % if only $\epsilon_b=0.6$ can be achieved. For the measurement of the top quark Yukawa coupling, $E_{\text{c.m.}}=1$ TeV is clearly far superior to $E_{\text{c.m.}}=500$ GeV for $m_H>100$ GeV.

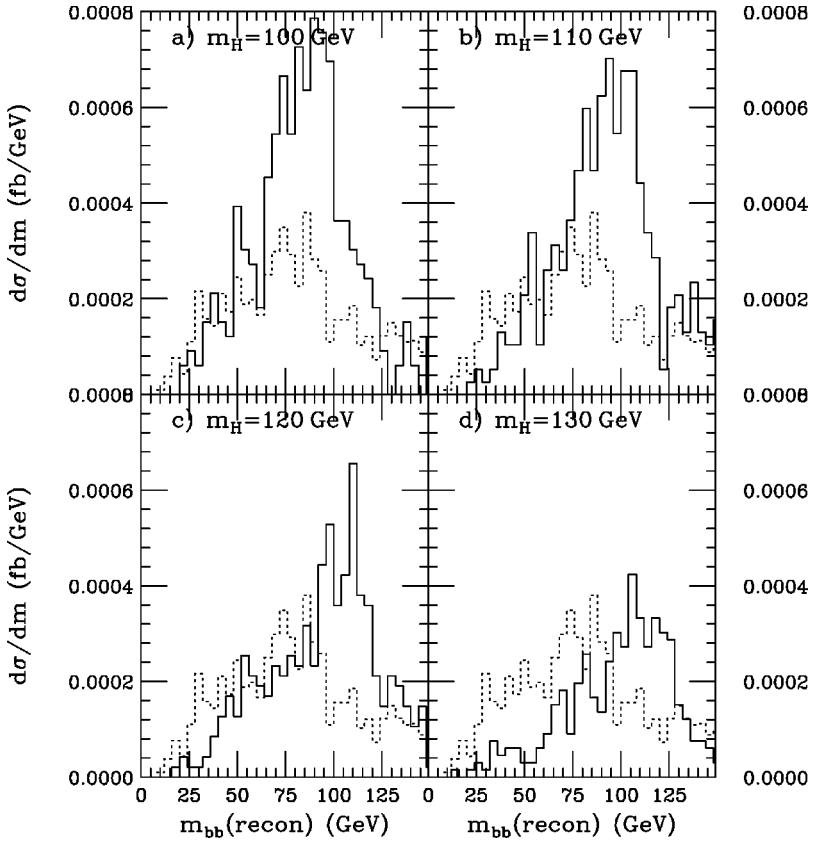

FIG. 10. Distribution in $b\bar{b}$ invariant mass for the two remaining b jets after top quark mass reconstruction in hadronic events at $E_{\text{c.m.}}=1$ TeV. The signal is solid, while the sum of EW and QCD backgrounds is dashed.

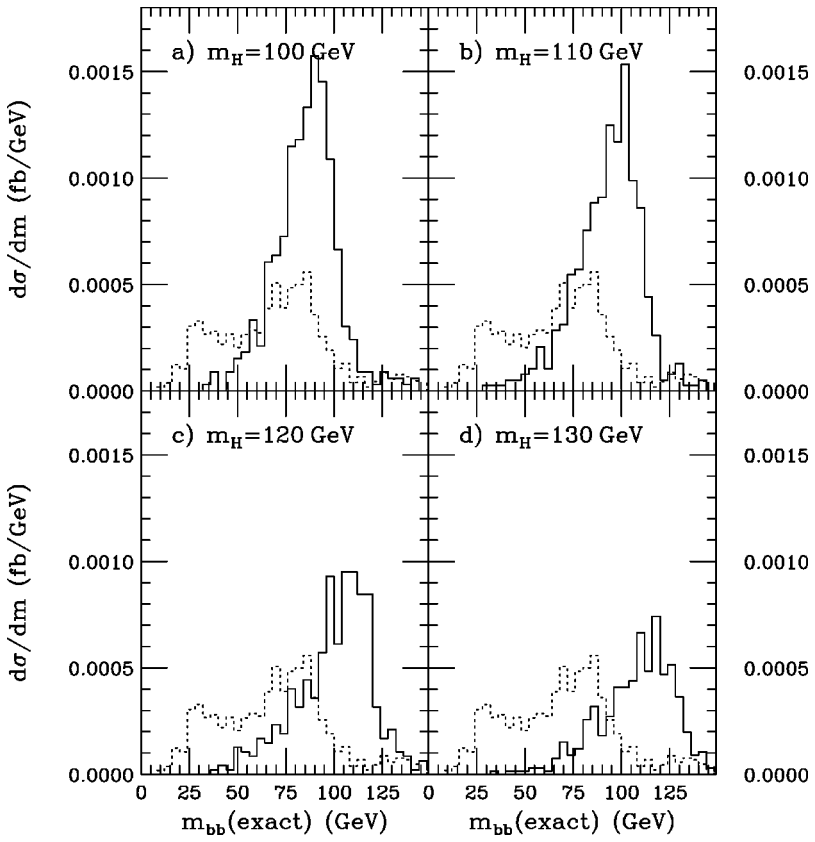

FIG. 11. Distribution in $b\bar{b}$ invariant mass for the two correctly identified non-top-quark b jets, using generator information for hadronic events, for $E_{\text{c.m.}}=1$ TeV. The signal is solid, while the sum of EW and QCD backgrounds is dashed.

B. Hadronic channel

Finally, we present results for the hadronic channel at $E_{\text{c.m.}}=1$ TeV. For this case, we apply again the same cuts as in Sec. III, but without the cut on E_b(slow). The results are given in Table VII. The reconstructed $m(bb)$ and exact $m(bb)$ are shown in Figs. 10 and 11. The corresponding results after applying a cut on $m(bb)$ are again listed in Table VII and range from 20 to 50 events for 1000 fb^{-1} of data. The precision on the top quark Yukawa coupling is given in Table VIII. The precision ranges from 10% to 14% for $\epsilon_b=1$ and from 28% to 39% if only $\epsilon_b=0.6$ is achieved.

V. CONCLUSIONS

The process $e^+e^-\to t\bar{t}H$ directly measures the $t\bar{t}H$ Yukawa coupling. We have computed the signal and the major backgrounds for both the semileptonic and hadronic decay channels using ISAJET to simulate gluon radiation, hadronization and decays. In our analysis, we rely on a direct reconstruction of the W, t and H masses in the events. At $E_{\text{c.m.}}=500$ GeV, even with 1000 fb^{-1} of integrated luminosity, only $m_H\lesssim 110$ GeV will give enough of an event rate for a reasonable measurement of the top quark Yukawa coupling. At higher energies, the entire range of $m_H=100$–130 GeV should be accessible.

Our final results indicate the statistical error that can be achieved on the measurement of the top quark Yukawa coupling. Systematic errors will also be present, but these will depend in detail on properties of the machine and detector, so we do not attempt to estimate these. Our final results can be quoted by combining the best measurement in the semileptonic channel with the best measurement in the hadronic channel, as two independent measurements. We then find for $\delta\lambda_t/\lambda_t$ at $E_{\text{c.m.}}=500$ GeV and 1000 fb^{-1},

m_H (GeV)	$\epsilon_b=1$	$\epsilon_b=0.6$
100	0.08	0.22
110	0.12	0.32
120	0.21	0.59
130	0.44	1.22

TABLE VIII. The $4b+\geqslant 4$ jets channel at $E_{\text{c.m.}}=1$ TeV: estimated error in the top quark Yukawa coupling ($\delta\lambda_t/\lambda_t$), assuming 10^3 fb^{-1} of integrated luminosity and $\epsilon_b=1$ ($\epsilon_b=0.6$).

Channel	$H(100)$	$H(110)$	$H(120)$	$H(130)$
$4b+\geqslant 4$ jets	0.10 (0.29)	0.11 (0.30)	0.13 (0.36)	0.17 (0.48)
$m(\text{rec})>65$	0.11 (0.30)	—	—	—
$m(\text{rec})>75$	—	0.11 (0.32)	—	—
$m(\text{rec})>90$	—	—	0.14 (0.39)	—
$m(\text{rec})>95$	—	—	—	0.18 (0.50)
$m(\text{ex})>65$	0.10 (0.28)	—	—	—
$m(\text{ex})>75$	—	0.10 (0.28)	—	—
$m(\text{ex})>90$	—	—	0.11 (0.32)	—
$m(\text{ex})>95$	—	—	—	0.14 (0.38)

while $\delta\lambda_t/\lambda_t$ at $E_{\text{c.m.}}=1$ TeV and 1000 fb^{-1} is

m_H (GeV)	$\epsilon_b=1$	$\epsilon_b=0.6$
100	0.06	0.17
110	0.06	0.18
120	0.07	0.19
130	0.08	0.22.

Our results qualitatively agree with those presented in Ref. [9], if we assume $\epsilon_b=1$. A high efficiency b tag, along with of order 1000 fb^{-1} of integrated luminosity, will be critical for the top quark Yukawa coupling measurement.

ACKNOWLEDGMENTS

The work of H.B. and L.R. was supported in part by the U.S. Department of Energy under Contract No. DE-FG02-97ER41022. The work of S.D. was supported by the U.S. Department of Energy under Contract No. DE-AC02-76CH00016. We are grateful to Frank Paige and Horst Wahl for valuable discussions.

[1] A. Djouadi, J. Kalinowski, and P. Zerwas, Z. Phys. C **54**, 255 (1992).
[2] E. Accomando *et al.*, Phys. Rep. **299**, 1 (1998).
[3] Delphi and L3 reports, Moriond meeting on ''Electroweak interactions and Grand Unified Theories,'' 1999.
[4] See e.g. J. Erler and P Langacker, hep-ph/9809352, 1998.
[5] See e.g. S. Heinemeyer, W. Hollik, and G. Weiglein, Phys. Lett. B **455**, 179 (1999); H. Haber, hep-ph/9901365, 1999.
[6] S. Moretti, Phys. Lett. B **452**, 338 (1999).
[7] S. Dawson and L. Reina, Phys. Rev. D **59**, 054012 (1999).
[8] S. Dittmaier, M. Kramer, Y. Liao, M. Spira, and P. Zerwas, Phys. Lett. B **441**, 383 (1998).
[9] A. Juste and G. Merino, ILCW Sitges 99 presentation.
[10] M. Sachwitz, S. Shichanin, and H. Schreiber (work in progress), as reported by G. Merino in [9].
[11] S. Dawson and L. Reina, Phys. Rev. D **60**, 015003 (1999).
[12] B. Grzadkowski, J. Gunion, and J. Kalinowski, Phys. Rev. D **60**, 075011 (1999).
[13] T. Stelzer and W. F. Long, computer code MADGRAPH, Comput. Phys. Commun. **81**, 357 (1994).
[14] H. Murayama, I. Watanabe, and K. Hagiwara, computer code HELAS, Report No. KEK-91-11, 1992.
[15] F. Paige and S. Protopopescu, computer code ISAJET, in *Supercollider Physics*, edited by D. Soper (World Scientific, Singapore, 1986), p. 41; F. Paige, S. Protopopescu, H. Baer, and X. Tata, hep-ph/9804321, 1998.